Study on the Morphology Structure and Properties of Aqueous Polyurethane Modified by Poly(dimethyl siloxane)

Liu Jiao, Pan Zhaoqi, Gao Yun

College of Material Science and Engineering, East China University of Science and Technology, Shanghai 200237, China

Received 2 October 2006; accepted 26 December 2006
DOI 10.1002/app.26371
Published online 17 May 2007 in Wiley InterScience (www.interscience.wiley.com).

ABSTRACT: In this study, a series of aqueous polyurethane modified by poly(dimethyl siloxane) PDMS were synthesized, which were based on polyoxytetramethylene glycol (PTMG), isophorone diisocyanate (IPDI), dimethylol propionic acid(DMPA), and PDMS. The copolymer was characterized by FTIR and the fraction of hydrogen bonded carbonyl group was determined through decomposition of C=O stretching. Energy dispersive X-ray analyzer (EDX) was used to investigate the siloxane concentration on the surface and bulk regions. The morphology of aqueous polyurethane before and after modification was studied by SAXS, including the interface between soft and hard micro-domain, the size and shape of the dispersive particles, as well as the degree of the phase separation. Influence on the morphology structure of aqueous polyurethane in different type and content of organic silicone was studied. It was shown that the degree of hydrogen bonding and phase separation of aqueous polyurethane decreased after the introduction the PDMS resulted from the migration of PDMS to the surface of the film. Therefore, water resistance improved a lot after the introduction of PDMS with different structures, and the tensile strength and elongation of APDMS(PDMS terminated by hydroxyalkyl) decreased while those of EPDMS(PDMS terminated by hydroxyl polyether) appeared little increase at low content and than decreased. J Appl Polym Sci 105: 3037–3046, 2007

Key words: polyurethanes; polysiloxanes; morphology; structure–properties relation; SAXS

INTRODUCTION

Polyurethane is an interesting class of copolymer because its excellent mechanical properties contributed to the formation of a microphase separation, consisting of hard-segment-rich domain, soft-segment-rich matrix, and interphase between them. The hard domains act as filler materials in soft segments matrix and provide filler-like reinforcement to the soft segment matrix.

It is widely known that research and development of aqueous polyurethane has been motivated by environmental considerations to reduce solvent emissions or even solvent free. However, because of the introduction of hydrophilic extender, aqueous polyurethane has to be modified to improve its water-resistance. Recently, interest in modification on aqueous polyurethane to improve its water resistance and surface properties has been mainly focus on PDMS, which possesses several interesting properties including low T_g, low surface energy (that can easily transfer around on the surface of the polymer and provide good hydrophobicity), and high stability, and so forth.[1–6] It has been widely reported that, because of the large difference between the solubility parameter of the nonpolar PDMS and high polar polyurethane, segmented PDMS–PU copolymers, where PDMS as soft segments demonstrated excess degree of micro phase separation, yielded relatively poor mechanical properties;[7] therefore, a number of methods have been demonstrated to improve the phase mixing of these materials, including use of blended soft segments of PDMS and polyether-diol.[8] Since it could decrease the degree of phase separation, the introduction of small PDMS content to PU, whose soft segment was pure polyether-diol, should influence the micromorphology structure including the degree of micro-phase separation. Therefore, it is very interesting to study the micromorphology structure of polyurethane system modified by organic silicone, and it is meaningful to analyze and control bulk properties of the material.

The detailed domain morphology of the materials and its main parameters can be characterized by small-angle X-ray scattering (SAXS).[9] Careful application of SAXS analysis provides measurements of

Correspondence to: G. Yun (gaoyun@shec.gov.cn).

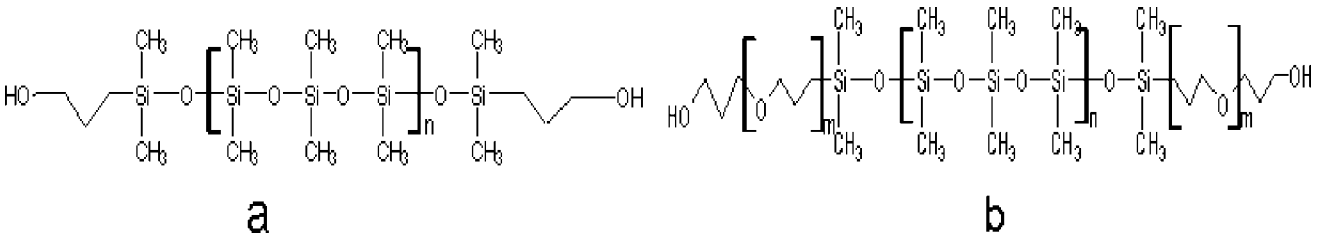

Scheme 1 Structure of PDMS; a: APDMS, b: EPDMS ($m/n \approx 1/2$).

interdomain space, the shape of the scattering particle (hard domains), the diffuse phase thickness, and degree of phase separation.

In this study, a series of polyether aqueous polyurethane modified by different PDMS which terminated by (hydroxyalkyl and hydroxyl polyether) are synthesized. The structure was characterized by FTIR and the degree of hydrogen bonding was investigated through decomposition of C=O stretching in infrared spectrum. The morphology was investigated by SAXS and confirmed by AFM, which provided advantage evidence to the analysis and control the bulk properties. In addition, a micromorphology structure model is proposed based on the results of measurements and analysis, which provides reasonable explanations for the effects of morphology on bulk properties of the modified materials.

SAXS analysis

SAXS could provide information on the morphology of a two-phase system when the domain sizes are on the order of nanometers and the electron density of the two phases differ sufficiently.[10]

SAXS analysis on the parameters of morphology structure in our study were taken under the scattering theory and experimental results reported by antecessors.[9,11]

The simplest of these analyses involves the applications of Bragg's equation[12] to determine interdomain space, sometimes called the ''long period,'' which can be obtained from:

$$d = 2\pi/q_{mex} \tag{1}$$

where q is the scattering vector and is defined as follows:

$$q = 4\pi(\sin\theta)/\lambda \tag{2}$$

where θ is an half of the scattering angle and λ is the wavelength of radiation.

q_{max} denotes the value of q at the peak of the scattering profile: the $I(q)$ versus q plot, which is always substituted by $I(q)q^2$ versus q plot after Lorentz correction.[13]

When the scattering profile is extrapolated to infinite scattering vector, for two phase structure with sharp phase boundaries, the Porod's law[14] is given by:[15]

$$\lim_{q\to\infty} \mathrm{l}(q) = \frac{K}{q^4} \tag{3}$$

However, real systems contain two structure features, which leads to deviations from this law. The existence of diffuse phase boundaries will contribute to negative deviations from Porod's law; then the corresponding Porod's law relation is:[16]

$$\lim_{q\to\infty} \mathrm{l}(q) = \frac{KH^2(q)}{q^4} \tag{4}$$

Where $H(q)$ is the Fourier transform of a function, which accounts for smoothing of the phase boundaries. Equation (5)[9]could be obtained from Eq. (4) given by

$$\ln\,[q^4|(q)] = \ln K - 1/2\ \sigma\ ^2q^2 \tag{5}$$

According to (5), interphase thickness E[9] related to σ is obtained by the slop of the plot ln $[I(q)^*q^4]$

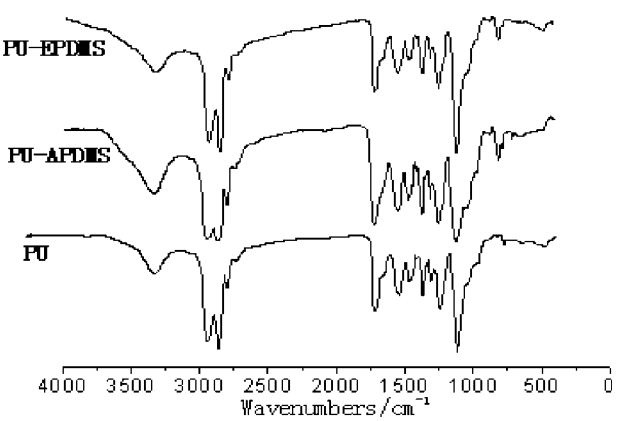

Figure 1 FTIR spectra of PU and PU-PDMS.

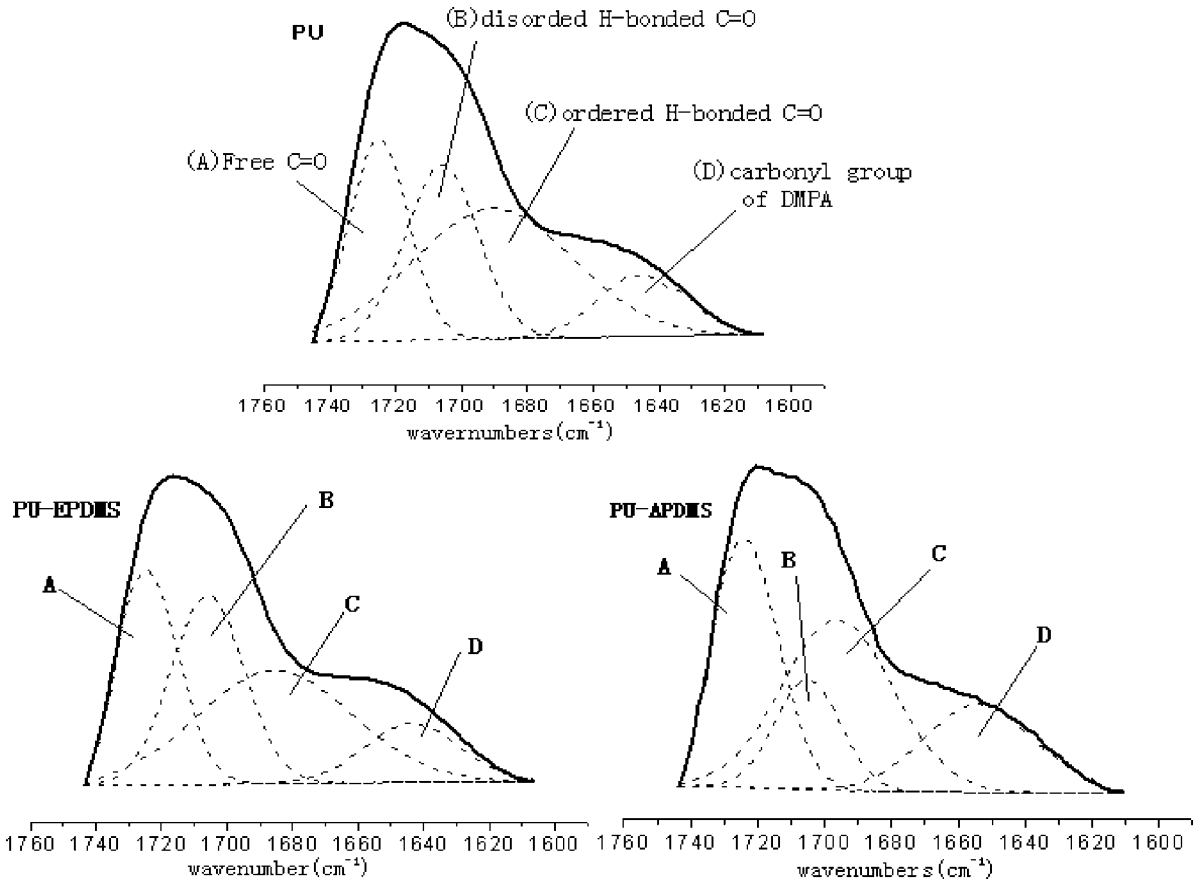

Figure 2 Decomposition of C=O stretching for PU and PU-PDMS samples.

versus q^2. Then $I(q)$ is amended to be $I(q)'$ through:[17]

$$\ln [q^4|'(q)] = \ln [q^4|(q)] + \sigma\ ^2q^2 \tag{6}$$

Other parameters of morphology are the shape and size of domains, which may be obtained by extrapolating the scattering profile to zero based on Guinier's law[18] given by:

$$I'(q) = I_eN^2 \exp(-q^2R_g/3) \tag{7}$$

where I_e is scattering intensity of single electron, N is the number of electrons in one scattering domains, R_g is gyroidal radius of domains, which reflects the average size of them. The plot of ln $I(q)'$ vs. q^2 according to Eq. (8) is a linear with the slop whose value is $R_g/3$.[18]

$$\ln I'(q) = \ln (I_eN^2) - q^2R_g/3 \tag{8}$$

The last parameter DPS (the degree of overall phase separation) is reflected in ratio (9):[9]

$$\mathrm{DPS} = \Delta\rho^2/\Delta\rho_c^2 \tag{9}$$

$\Delta\rho_C^2$ is the variance in electron density for an ideal two phase system, defined as:[9]

$$\Delta\rho_c^2 = \phi_1\phi_2(\rho_1 - \rho_2) \tag{10}$$

Where φ_i and ρ_i are the volume fraction and electron density of ith phase, respectively. This value

TABLE I
Decomposition Results of C=O Stretching

	Peak position (cm^{-1})					Fraction of peak area				
Sample	Total	Free C=O	Disordered H-bonded C=O	Ordered H-bondeded C=O	C=O of DMPA	Free C=O	Disordered H-bonded C=O	Ordered H-bondeded C=O	C=O of DMPA	X_b
PU	1709	1725	1706	1690	1646	0.22	0.26	0.42	0.10	0.68
PU-EPDMS	1710	1725	1706	1686	1644	0.29	0.27	0.34	0.10	0.61
PU-APDMS	1713	1724	1701	1689	1646	0.35	0.17	0.37	0.11	0.51

TABLE II
EDX Result for PU-APDMS

	Relative percent of atom/%			
	O	N	C	Si
Surface	24.51	2.04	72.20	1.25
Bulk	22.62	2.59	74.55	0.24

may be calculated from the known chemical composition and densities of the component phases by assuming complete phase separation. However, $\Delta\rho^{2\prime}$ is the real experimental electron density variance with the presence of mixing within phases and diffuse boundaries. It is defined as follows:[9]

$$\Delta\rho^{2\prime} = \frac{1}{2\pi^2 i_e}\int_0^\infty I(q)'q^2 dq \tag{11}$$

The above integral may be calculated through extrapolation of measured scattering profiles. Then $\Delta\rho^2$ may be obtained as well as DPS.

EXPERIMENTAL

Materials

Polyoxytetramethylene glycol (PTMG, M_w = 2000 g mol^{-1}, OH number = 112 mg of KOH per gram; HuaDa Chemical Corp. Yantai, China); isophorone diisocyanate (IPDI, Degussa-Hus). Dimethylol propionic acid (DMPA, Perstorp Polyols Inc.); enylene diamine (EDA, AR, Xingzhen Chemicals First Factory, China)); acetone and *N*-methyl-2-ketopyrrolidine(NMP, distilled before use), triethylamine(TEA, AR, Xingzhen Chemicals First Factory, China), stannous laurate as catalyzer. APDMS(PDMS terminated by —CH_2—CH_2—OH, M_n = 2000, DeYi Chemical, Shanghai, China), EPDMS(PDMS terminated by —(CH_2—CH_2—CH_2—O)*n*—CH_2—CH_2—OH, M_n = 2000, DeYi Chemical, Shanghai, China), the detailed structure of the PDMS is showed in Scheme 1.

PDMS segmented aqueous polyurethane synthesis

Reaction was carried out under a nitrogen atmosphere in four-necked round-bottomed flask with a mechanical stirrer, thermometer, condenser and dropping funnel. An oil bath was used to control the temperature. The stoichiometric IPDI was first added to the flask. Stirring was then started and heated the material to about 60°C. DMPA resolved in NMP was added and the reaction at 60°C was kept about 1 h. Catalyst was then added and the temperature was raised to 80°C. Stoichiometric PTMG and PDMS were added to the system and kept it under 80°C for 3 h. The progress of the reaction was controlled by titration to determine the content of NCO in the system. Then the temperature of the system was allowed to fall to 50°C and the carboxylic acid groups were neutralized by addition of TEA. A little acetone was added to decrease the viscosity of the prepolymer. The mixture was stirred for further 60 min to ensure the neutralized reaction completed. After this step, with the addition of prepolymer to water and EDA to the mixture, the reactions of dispersion and chain extending completed by stirring for about 30 min.

Film samples preparation

Certain mass emulsion was put into the glass model and allowed to dry at room temperature for about 48 h. The polyurethane cast films were obtained after staying at oven about 3–4 h under 60–100°C and at vacuum oven for 24 h under 80°C. The thickness of the cast films were about 0.3–0.5 mm.

Characterization

FTIR result was obtained using a Electron Nicolet 5700 FTIR spectrometer using solvent (THF) cast film

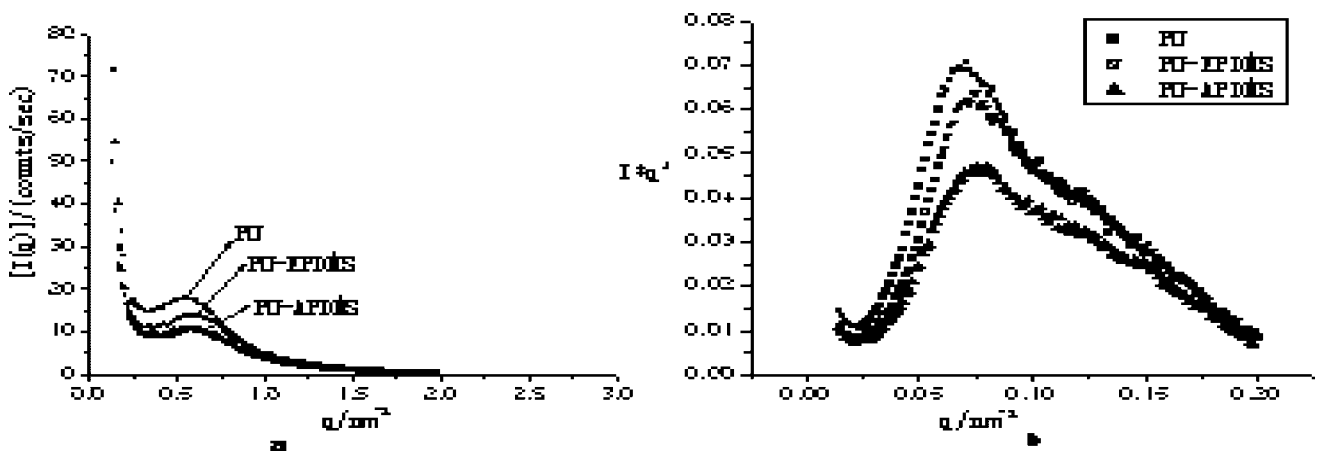

Figure 3 Scattering profiles for PU modified by different PDMS.

TABLE III
SAXS Calculated Results for PU Modified by different PDMS

Sample	q_{max} (nm^{-1})	d (nm)	E (nm)	R_g (Å)	$\Delta\rho^{2'}$	$\Delta\rho_C{}^2$	DPS
PU	0.07112	88.30	16.0	96	0.01589	0.00653	0.41
PU-EPDMS	0.07397	84.90	16.3	64	0.01616	0.00591	0.36
PU-APDMS	0.07539	83.30	15.0	56	0.01649	0.00477	0.28

on KBr discs. SAXS experiments were taken at room temperature, on a Nanostar U small-angle X-ray scattering system (Bruker, Germany), using Cu-Kα radiation (wavelength = 0.154 nm, 40 KV, 35 mA) and pinhole collimation system; all the data were corrected for background. AFM experiments were taken at American DI nanoscope IIIA system, using multimode. SEM-EDX experiments were taken on JEOL JSM-6360LA SEM system and EX-23000BUB energy dispersive X-ray analyzer. Tensile test for the films were carried out using CMT tensile tester at room temperature and the tensile speed was 500 mm min^{-1}.[19] Water resistance of the films was determined by the weight for 48 h. The weights of samples before and after soaking in water were signed as m_1 and m_2, respectively. Rate of water absorption A used to determine the water resistance was defined as follows:

$$A = [(m_2 - m_1)/m_1]100\% \quad (12)$$

RESULTS AND DISCUSSION

FTIR result

The typical FTIR-ART spectra of PU and PU-PDMS is showed in Figure 1. With the introduction of PDMS, the intensity of the peak around 1080–1100 cm^{-1}(C—O—C, Si—0—Si streching), 1260 cm^{-1}(CH_3 in Si—CH_3 sym.bending) and 803cm^{-1}(CH_3—Si rocking) increased, which indicated that the PDMS-PU copolymer formed.[20]

Infrared spectroscopy has been employed extensively to study the hydrogen bonding and is a useful tool for characterizing the characteristics of hydrogen bonding in domains.[21–23] The frequency of hydrogen bonded groups are lower than the corresponding free groups(i.e. C=O in PU structure). It has reported[24,25] that the peaks around 1610–1740 cm^{-1} showed in Figure 1 were the composition of C=O stretching including stretching of free urethane carbonyl groups around 1725 cm^{-1}, whereas the urethane carbonyl stretching around 1710 cm^{-1} is due to hydrogen bonding in disordered regions, which is attributable to the carbonyl participating in the urethane linkage of interfacial regions or being dissolved in the soft phase, the stretching of the stronger hydrogen bonds at a lower frequency around

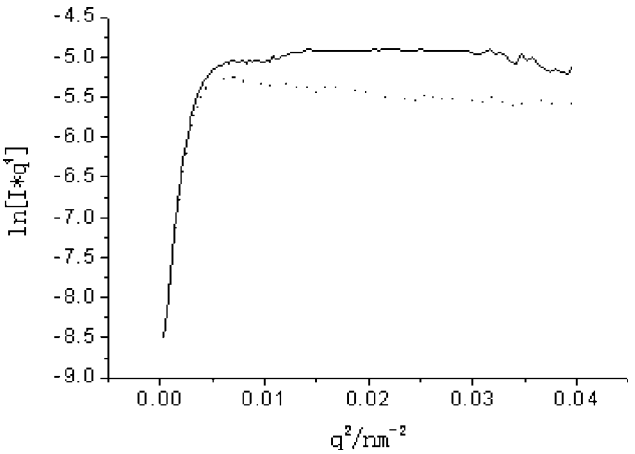

Figure 5 Porod' s law curves for PU.

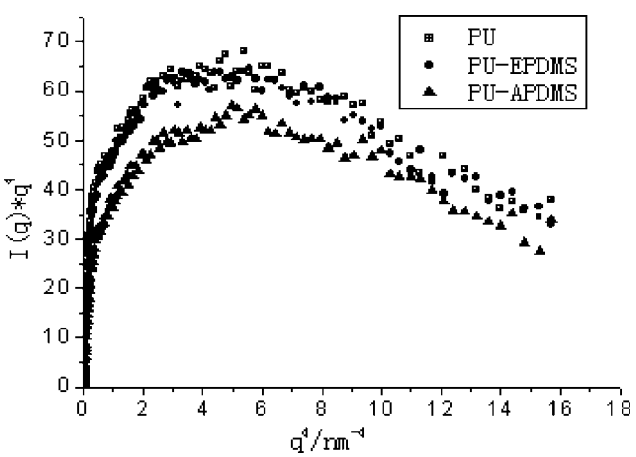

Figure 4 Typical Porod' s law curves with the negative deviation.

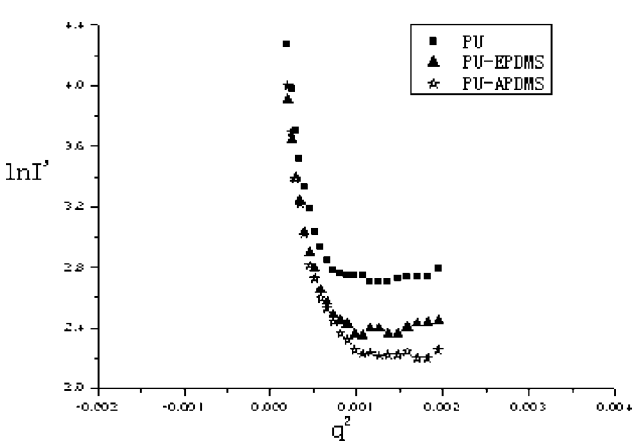

Figure 6 Guinier curves for PU modified by different PDMS.

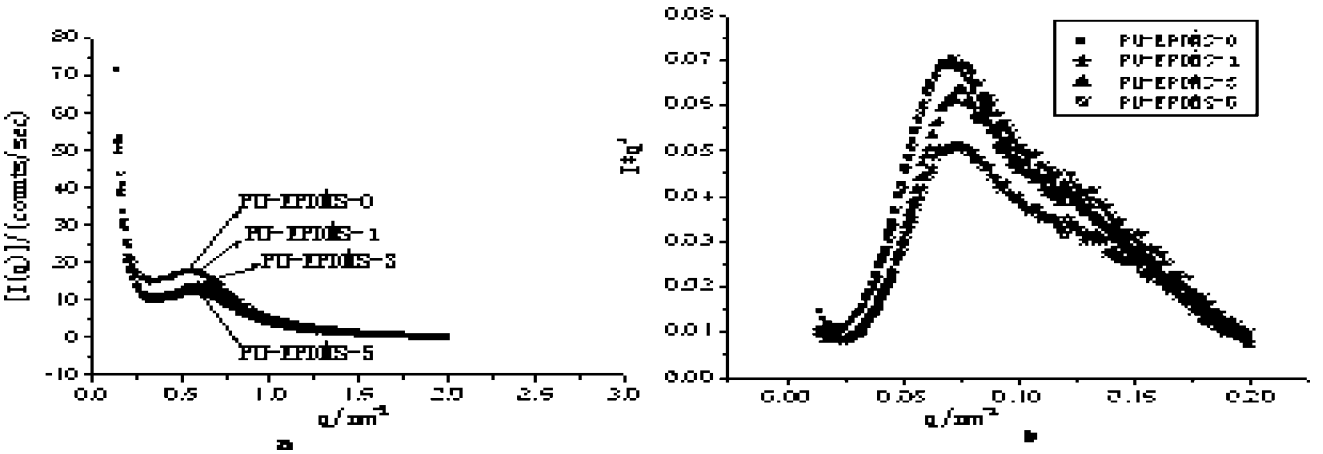

Figure 7 Scattering intensity plot of PU and PU-PDMS.

1695 cm^{-1} in ordered or crystalline regions and the stretching of hydrogen-bonded carboxylic carbonyl groups, which come from the DMPA unit near 1665 cm^{-1}.

The spectra were analyzed with a curve-resolving technique based on linear least-squares analysis to fit the combination of Lorentzian and Gaussian curve shapes.[26] Curve fitting of the C=O stretching region was performed for all samples. Figure 2 shows the results of the curve fitting procedure for PU and PU-PDMS samples with various types of PDMS to investigate the degree of hydrogen bonding.

The total fraction[22] of the carbonyl absorption group participating in hydrogen bonding is expressed as $X_b = S_b/S_t$, where S_t is the total peak area of carbonyl groups and S_b is the peak area of hydrogen-bonded carbonyl groups. The results were listed in Table I.

The results showed the disordered the H-bonded C=O decreased when the APDMS was introduced, while that of PU-EPDMS changed a little, which indicated that the interphase thickness was thinner in the former and changed a little in the latter one.[24,25] From the fact that the ordered H-bonded C=O decreased a lot in the both modified samples, may demonstrate the hard domains concentrated less than unmodified sample. Value of X_b decreased after the modification, which may low the cohesive energy of the system and decreased the strength of the material.

SEM-EDX result

Table II shows the results of SEM-EDX for the PU-PDMS samples.

Table II showed that percent of atom Si in the surface of film was much larger than that in the bulk of the film. It indicated that the most of siloxane migrated to the surface of the film due to its low surface energy. Since the PDMS was introduced to the backbones of the PU structure, the trend of the migration may influence the formation of ordered H-

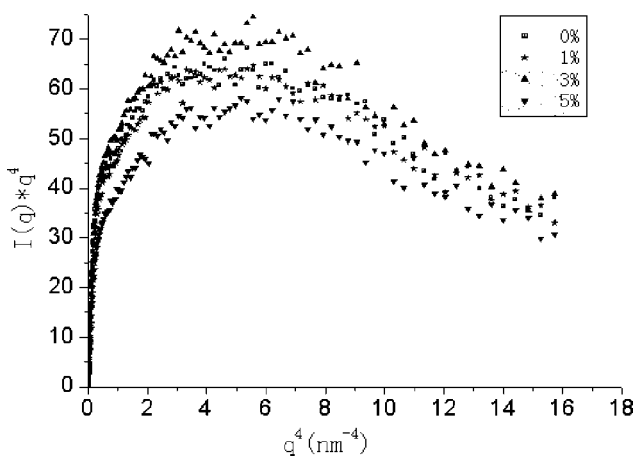

Figure 8 Typical Porod' s law curves with the negative deviation.

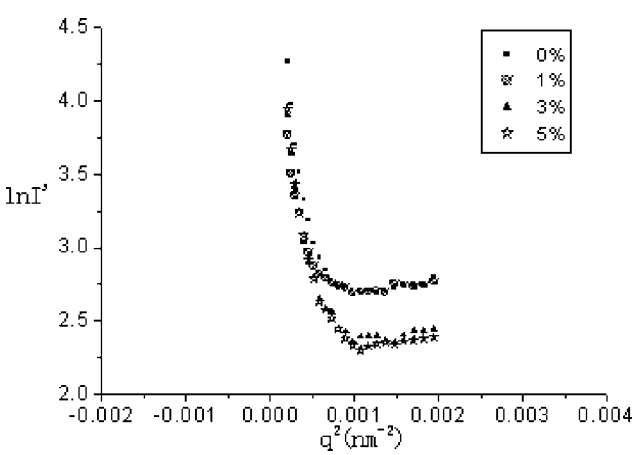

Figure 9 Guinier curves for PU modified by different content of EPDMS.

TABLE IV
SAXS Calculated Results for PU Modified by Different Content of EPDMS

Content of EPDMS	q_{max} (nm^{-1})	d (nm)	E (nm)	R_g (nm)	$\Delta\rho^{2'}$	$\Delta\rho_C{}^2$	DPS
0%	0.07112	88.30	16.0	96	0.01589	0.00653	0.41
1%	0.07255	86.56	16.2	94	0.01600	0.00667	0.41
3%	0.07397	84.90	16.3	64	0.01616	0.00591	0.36
5%	0.07539	83.3	15.5	60	0.01634	0.00512	0.31

bonding and the congregation of the hard segments. It should ruin the micro structure of the samples. The change on the microstructure should be testified by the SAXS results. However the results may improve the water resistance a lot for the modified samples.

SAXS results for PU and PU-PDMS

Figure 3(a) shows the scattering profile of different samples $I(q)$ versus q, from which it could be obtained that these systems were microphase separation. The so-called Lorentz correction[13] by multiplying $I(q)$ with q^2 is showed in Figure 3(b).

q_{max} was obtained from Figure 3(b) and the interdomain spacing d calculated through Bragg Eq. (1): $d = 2\pi/q_{max}$ were listed in Table III.

Figure 4 shows the plot $I(q)^*q^4$ versus q^4[49] to find out the main effect on the deviation from Porod's law. It was implying the diffuse interphase exist and it made negative deviation from the Porod's law. The interphase thickness E obtained through (5), and the results were showed in Table III. The negative deviation was amended through (6) as shown in Figure 5 (take PU as an example) and the real intensity could be obtained to calculate other parameters.

After amendment, and Guinier curves of the samples before and after modification through (8) were showed in Figure 6:

According to (8), R_g of hard domains could be obtained by the slop of the linear when q tended to zero, as well as the length of the linear that reflected the symmetry of the hard domains. All the calculated results were listed in Table III.

DPS of the samples were calculated from eqs. (9)–(11) the results were also listed in Table III.

It indicated that the interdomain spacing, the size of hard domains and the degree of phase separation decreased after the modification. The influence was more on the PU-APDMS. The interphase thickness E of PU-EPDMS increased while that of PU-APDMS decreased. According to the results of H-bonding analysis, R_g decreased should due to the less ordered H-bonded C=O in the hard domains and make it difficult to congregate the hard segments to form the larger hard domains. The change on E were identified the fraction of disordered H-bonded C=O. Meanwhile, it demonstrated that the migration of siloxane really influenced the regular of the structure, thus the domains formation were difficult and resulted in a less degree of phase separation. The

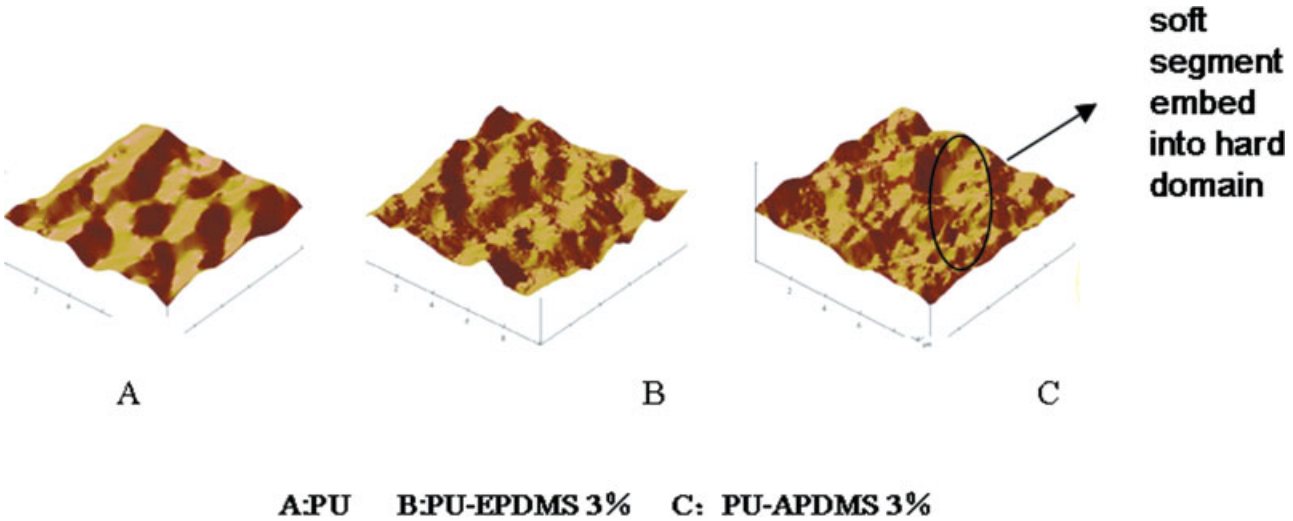

Figure 10 AFM for PU and PU-PDMS. [Color figure can be viewed in the online issue, which is available at www.interscience.wiley.com]

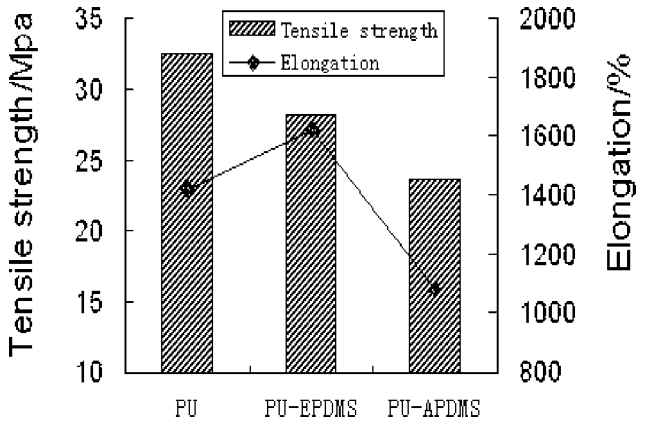

Figure 11 Mechanical property of PU and PU-PDMS.

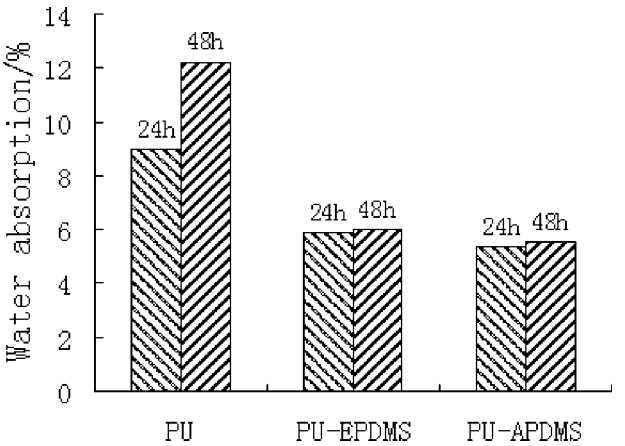

Figure 12 24 h and 48 h water absorption of PU and PU-PDMS.

different change happened on the different types of the PDMS should due to their different structure as showed in Scheme 1. The long polyether chains made the chains more flexible thus increase the possibility of contact between soft and hard segments and increased the interfacial regions. Additionally, less DMS chains made the smaller influence brought by the migration of siloxane.

SAXS results of PU films on different content of EPDMS

Figures 7–9 described the plots to obtain the morphology structure parameters including interdomain spaces d, interphase thickness E, the size of the hard domains R_g and the degree of phase separation DPS like those described above.

All the calculated results were listed in Table IV.

From Table IV it was found that d, R_g, and DPS decreased with the content of EPDMS increasing. However, the interphase thickness E increased when the EPDMS was very small while when the content increased to 5%, E was decreased. The results were due to the migration of the EPDMS to the surface because of its low surface energy. With the more content of EPDMS introduced to PU, the regular structure ruined more seriously. Also, the H-bonded system was changed to the different extent. However, because of its special structure, the migration of PDMS ruined the regularity and at the same time, it increased the flexibility of the chains and increased the contact between soft and hard segments thus increased E. The opposite effects were happened at the same time; therefore, the results demonstrated the integrative appearance.

AFM result of micromorphology

Figure 10 shows the AFM images of aqueous PU film before and after modification with different type of PDMS.

According to the principle of tapping mode of AFM operation, the light color areas in Figure 10 represented the micro-domain of hard segments, and the dark color areas correspond to the microdomain of soft segments.[27] Figure 10(A) shows the AFM image of pure PU film, micro-phase separation of soft segments and hard segments can be observed clearly. The congregating hard segments dispersed into the soft phase, but the size of hard segment microdomain is a little bit larger. Figure 10(B,C) shows the AFM images of PU modified by PDMS, microdomain of hard segments also dispersed into the soft phase, but the size of microdomain become smaller and more dispersedly. From Figure 10(C), part of soft segment embed into the microdomain of hard segment, because that the long PDMS segment of APDMS which is incompatible with hard segments was introduced into PU molecular backbone

TABLE V
Macroproperties of PU and PU-PDMS

Sample	Tensile strength (Mpa)	Elongation/%	Water absorption 24 h/%	Water absorption 48 h/%
PU	32.56	1419	8.89	12.21
PU-EPDMS	28.18	1625	5.88	6.02
PU-APDS	23.61	1081	5.34	5.52

TABLE VI
Macroproperties of PU in Different Content of EPDMS

Sample	Tensile strength (Mpa)	Elongation/%	Water absorption 24h/%	Water absorption 48h/%
PU	32.56	1419	8.89	12.21
PU-EPDMS-0.5	33.91	1457	7.21	7.72
PU-EPDMS-1	31.88	1459	6.13	6.23
PU-EPDMS-3	28.18	1625	5.88	6.02
PU-EPDMS-5	22.50	1608	5.7	5.91

chain and prevented the large microdomain of hard segments packing. All those were identical with the analysis results from SAXS.

Mechanical properties

Macroproperties of aqueous PU film in different type of PDMS

Figure 11 and Table V show that the pure aqueous PU film had excellent mechanical properties due to proper microphase separation, the tensile strength was about 32.56 MPa and the elongation at break was more than 1400%. The tensile strength was reduced after modification of PDMS, the elongation at break was improved with the modification of EPDMS, but decreased with the modification by APDMS.

According to analysis of SAXS, with the introduction of PDMS, the degree of phase separation and the hydrogen bonding between hard domains decreased and the cohesion energy in smaller hard domains was weaker, which may decreased the tensile strength of the materials. In addition, as resulted from SAXS analysis, the thinner interphase thickness *E* (APDMS) indicated the cohesive strength between soft and hard phase decreased, thus the function of hard domains as reinforcement were deceased, and the materials demonstrated lower tensile strength. However, thanks to the relative lower content of DMS and little larger interphase thickness compared to PU, mechanical properties of PU-EPDMS was relatively similar to those of PU, especially when the content of EPDMS was not large.

As to the water-resistance shown in Figure 12 and Table V, the water resistance of PU films increased greatly after modification due to the low surface energy of PDMS and its migration to the surface of the film, as well as the smaller and more dispersedly hard domains contained hydrophilic groups should contributed to nonexcess and nonmass absorption of water. However, when the introduction content of PDMS was the same, because of the longer DMS chains in APDMS, PU-APDMS demonstrated better water resistance.

Macroproperties of aqueous PU film in different content of EPDMS

Figure 13 and Table VI show that the tensile strength of aqueous PU film was decreased with increasing of content of PDMS while the elongation at break increased in low content.

The explanation for the Figures 13 and 14 and Table VI can be given on the basis SAXS results. On the one hand, the tensile strength was decreased

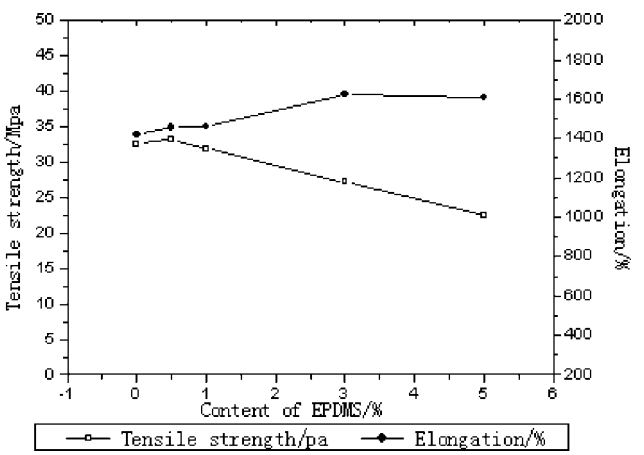

Figure 13 Mechanical properties of PU in different content of EPDMS.

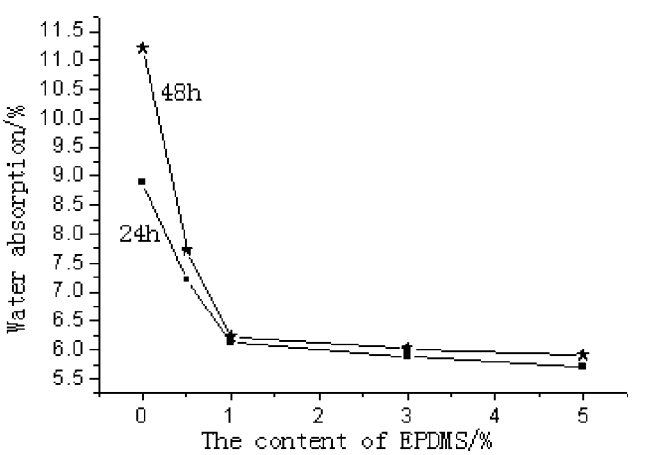

Figure 14 24 h and 48 h water absorption of PU-Si in different content of organic silicon.

mainly due to the less hydrogen bonding between hard domains and the decrease of DPS with the content of EPDMS increasing. On the other hand, the elongation at break was increased when the content was low given by the smaller hard domains and relative little increasing in interdomains thickness. However, when the content of PDMS to certain degree, the mechanical properties decreased, especially the elongation tended to decrease resulted from the introduction of more PDMS and the phase separation got the negative effect to the lower degree. The change happened on the mechanical properties proved that the introduction of PDMS to polyurethane should be controlled to a certain degree, though the water resistance was increasing with the PDMS content increasing to a certain content, (like more than 5%), mechanical properties would decrease while water resistance improve only a little, as it was showed in Figure 14. The results should be interpreted through the change of morphology structure that with the increase in PDMS content, the interphase thickness could not remain increasing due to the more DMS decreased the probability of hydrogen bonding between soft and hard segments as the results from FTIR analysis and the less regularity of the structure as the results from SAXS analysis.

CONCLUSIONS

The micro morphology structure particular the structure of hard domains of aqueous polyurethane was affected after the modification by PDMS. The incompatibility between the PDMS and hard segment of polyurethane and the migration of siloxane to the surface thus ruin the regular structure and hydrogen bond system should be the main reason to the change, After the modification by PDMS, the interdomain space, the size of hard domains decreased. The interphase thickness E, which should be the main point to the mechanical properties of the micro phase separation materials changed based on the different structure of PDMS. With the change happened on the structure parameters, the total degree of phase separation and the macro properties were effected which should demonstrate the integrated results.

The purpose to improve the water resistance has been obtained since after the introduction of PDMS, the water absorption could decrease to less than 6% or even lower than it. According to the mechanical properties, in our system EPDMS should be the reasonable choice for the modification for its relative less effect thanks to its special structure. However, the content of the EPDMS introduction should be controlled at a relative low value if mechanical properties are under the consideration.

References

1. Polmanteer, K. E.; Hunter, M. J. J Appl Polym Sci 1959, 1, 3.
2. Chen, H.; Fan, Q.; Chen, D. Z.; Yu, X. H. J Appl Polym Sci 2001, 79, 295.
3. Fan, Q. L.; Fang, J. L.; Chen, Q. M.; Yu, X. H. J Appl Polym Sci 1999, 74, 2552.
4. Hill, D. J. T.; Killeen, M. I.; O'Donnell, J. H.; Pomery, P. J.; St. John, D.; Whittaker, A. K. J Appl Polym Sci 1996, 61, 1757.
5. Meng-Shung, Y.; Ping-Yuan, T. J Appl Polym Sci 2003, 90, 233.
6. Adhikari, R.; Gunatillake, P. A. J Appl Polym Sci 2002, 87, 1092.
7. Speckhard, T. A.; Cooper, S. L. Rubber Chem Technol 1986, 59, 405.
8. Gunatillake, P. A.; Meijs, G. F.; McCarthy, S. J.; Adhikari, R. J Appl Polym Sci 2000, 76, 2026.
9. Jeffrey, T. K. J Polym Sci Part B: Polym Phys 1983, 21, 1439.
10. Strobl, G. R.; Schneider, M. J. J Polym Sci Polym Phys Ed 1980, 18, 1343.
11. Mo, S.; Douglas, J. J Appl Polym Sci 2001, 79, 1958.
12. Tyagi, D. Polym Eng Sci 1986, 25, 1371.
13. Martin, D. J.; Meijs, G. F.; Renwick, G. M.; McCarthy, S. J.; Gunatillake, P. A.; Gordon, F. J Appl Polym Sci 1996, 62, 1383.
14. Porod, G. Kolloid Z 1951, 83, 124.
15. Mori, T. Kobunshi Ronbunshu 1983, 40, 767.
16. Samulski, T. V.; Samulski, E. T. J Chem Phys 1977, 67, 824.
17. Zhihong, L.; Yanyun, G.; Dong, W., et al. Microporous Mesocrous Mater 2001, 46, 75.
18. Guinier, A. Ann Phys 1939, 12, 161.
19. Baoming, L. The Handbook of Test Method for Plastic; Shanghai Science and Technology Literature Publishing: Shanghai, 1994.
20. Hong, C.; Quli, F.; Dongzhong, C.; Xuehai, Y. J Appl Polym Sci 2001, 79, 298.
21. Coleman, M. M.; Skrovanek, D. J.; Hu, J.; Painter, P. C. Macromolecules 1988, 21, 59.
22. Teo, L. S.; Chen, C. Y.; Kuo, J. F. Macromolecules 1997, 30, 1793.
23. Wen, T. C.; Wu, M. S. Macromolecules 1999, 32, 2712.
24. Sung, C. S. P.; Schneider, N. S. Macromolecules 1977, 10, 452.
25. Pollack, S. K.; Shen, D. Y.; Hsu, S. L.; Wang, Q.; Stidham, H. D. Macromolecules 1989, 22, 551.
26. Jung-Eun, Y.; Ju-Shik, K. J Appl Polym Sci 2002, 86, 2375.
27. Garrett James, T.; Siedlecki, C. A. Polymer Preprints 2001, 42, 689.